

# Modelling and Simulation of Fe<sub>2</sub>O<sub>3</sub>/Aluminum Thermite Combustion

Paulo Brito<sup>1,2\*</sup>, Luísa Durães<sup>2</sup>, José Campos<sup>3</sup>, António Portugal<sup>2</sup>

<sup>1</sup> Chem. Technol. Dept., School of Technol. and Manag., Bragança Polytechnic Inst., Campus de Santa Apolónia, 5301–857 Bragança, Portugal

<sup>2</sup> CEM Group, Chem. Eng. Dept., Univ. of Coimbra, Pólo II, 3030–290 Coimbra, Portugal

<sup>3</sup> Thermodynamics Group, Mech. Eng. Dept., Univ. of Coimbra, Pólo II, 3030–201 Coimbra, Portugal

**Keywords:** Combustion, Thermite, Modelling, Finite differences, Adaptive methods, Grid refinement  
**Topic:** Engineering Sciences and Fundamentals – Energy and Transport Phenomena.

## Abstract

We present a one-dimensional model to simulate self-propagating high-temperature synthesis processes. The radial combustion of Fe<sub>2</sub>O<sub>3</sub>/Al thermite is used as case study. The model considers non-steady propagation with conductive/radiative heat transfer mechanisms and zero order kinetics. The thermophysical properties of the components depend on the temperature and composition of the mixture and appropriate mixing rules are used for each property. Fixing the thermophysical properties for the initial conditions, we conclude that increasing  $K$  leads to higher maximum temperatures and wave propagation velocities, always with complete conversion. The simulation results are in good agreement with the experimental observations. The activation of the thermophysical properties variation causes numerical difficulties which are being solved by further tuning of the parameters.

## 1 Introduction

The self-propagating high temperature reactions, as the Fe<sub>2</sub>O<sub>3</sub>/Al thermite combustion, present singular characteristics, which make them hard to follow by experimentation, namely the generation of a significant number of intermediary chemical species and structures, the fast chemical and physical transformations and the high temperatures achieved. Consequently, the studies concerning theoretical prediction of these processes can be a valuable guideline for experimental work and many publications have arisen in this area (Makino, 2001, Moore and Feng, 1995, Norozhilov, 1992).

Models for the simulation of combustion processes are a class of algebraic-differential problems which solution is characterised by steep thermal fronts propagating with highly non-linear dynamics. The front propagation modes can be complex (front pulsation, rotational propagation, etc) and instability features often appear when the parameters values lie beyond critical limits. The modelling strategies are based in a wide variety of approaches to problems differing in several characteristics (Ivleva and Merzhanov, 2000, Raymond et al., 1998, Shkadinsky et al., 2000, Volpert et al., 1992): geometry of the samples (cylindrical, rectangular, disk shaped), number of considered spatial coordinates (one-, bi- or three-dimensional), preferential propagation direction (axial or/and radial); assumed propagation regime (quasi-steady or transient), and the physico-chemical assumptions for the reactive system (components relative movement, phase transitions, presence of gases or particles, reaction mechanisms and kinetics). The studies may consider the analytical solutions of highly simplified models or solve the models using numerical integration methods. Due to the extreme process conditions and the great uncertainty on parameters estimation, these problems are interesting case-studies to test a variety of adaptive numerical methods for differential systems integration.

In this work, we construct and solve a model to simulate self-propagating high-temperature synthesis processes, using the Fe<sub>2</sub>O<sub>3</sub>/Al thermite as case study. It has already been simulated in cylindrical geometry with a one-dimensional coordinate system attached to the uniformly propagating combustion

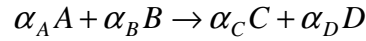
---

\* Corresponding author. Tel + 351-239-798737. E-mail:brito@eq.uc.pt

wave (Raymond et al., 1998, Shkadinsky et al., 2000, Shkadinsky et al., 1997), and with a fixed one-dimensional coordinate system (Brito et al., 2004). However, the availability of experimental results of radial combustion on disk shaped samples (Durães et al., 2005) has stimulated the derivation of a model to describe the combustion radial propagation. The built model congregates several features of simpler models published (Bowen and Derby, 1995, Carrillo-Heian et al., 1999, Cuadrado-Laborde et al., 2003, Graeve et al., 2001). We apply adaptive numerical methods in the resolution, involving several mesh adaptation methods based on continuous grid refinement techniques (Brito, 1998).

## 2 Model

In this work, we construct a one-dimensional model to simulate the propagation of a radial combustion wave. It is considered a general chemical reaction with the following massic stoichiometry:



The model considers non-steady propagation with conductive/radiative heat transfer mechanisms and zero order kinetics reaction. Based on these assumptions we derived the energetic balance, considering: disk shaped sample with radius  $R$  and thickness  $Z$ , sample confined in a steel cup with a PMMA top lid, negligible relative movement between species, limiting reactant A. It was obtained:

$$\rho_M C_{PM} \frac{\partial T}{\partial t} = \frac{1}{r} \frac{\partial}{\partial r} \left( k_M r \frac{\partial T}{\partial r} \right) + Q \mathbf{r} - \left[ (U_{steel/air} + U_{PMMA/air})(T - T_0) + 2\sigma \varepsilon_M (T^4 - T_0^4) \right] / Z \quad (1)$$

where subscript  $M$  stands for the mixture. The last term quantifies the heat losses to the surrounding (at  $T_0$ ) by the sample top and bottom faces.  $\sigma$  is the Steffan-Boltzman constant and  $\varepsilon$  the emissivity.

The mass partial balance for reactant A takes the form:

$$\frac{dW_A}{dt} = \alpha_A \mathbf{r} \quad (2)$$

where  $W_A$  is the mass concentration of A.

The simultaneous resolution of the differential equation system (1) and (2) gives the temperature and composition spatial and temporal profiles. Using the reactant A conversion,

$$\eta_A = \frac{W_{A0} - W_A}{W_{A0}} \quad (3)$$

the concentrations of all the species are computed:

$$W_B = W_{B0} - \frac{\alpha_B}{\alpha_A} \eta_A W_{A0} \quad (4); \quad W_C = W_{C0} - \frac{\alpha_C}{\alpha_A} \eta_A W_{A0} \quad (5); \quad W_D = W_{D0} - \frac{\alpha_D}{\alpha_A} \eta_A W_{A0} \quad (6)$$

The differential problem is completed by the definition of suitable initial and boundary conditions. The initial conditions for the temperature and mass concentration of A over the spatial domain are:

$$t = 0; \quad R_0 \leq r \leq R \Rightarrow T = T_0; \quad W_A = W_{A0} \quad (7)$$

A temperature pulse perturbation with height  $T_{igni}$  and length  $t_{igni}$  was considered to simulate the ignition on the inner boundary:

$$0 < t < t_{igni}; \quad r = R_0 \Rightarrow T = T_{igni} \quad (8); \quad t \geq t_{igni}; \quad r = R_0 \Rightarrow T = T_0 \quad (9)$$

Finally, we consider conductive/radiative heat transfer on the external boundary:

$$t > 0; \quad r = R \Rightarrow k_M \frac{\partial T}{\partial r} = - \left[ U'_{steel/air} (T - T_0) + \sigma \varepsilon_M (T^4 - T_0^4) \right] \quad (10)$$

The reaction enthalpy is computed considering the enthalpy variations at constant pressure of reactants and products between the reference temperature  $T_0$  and the temperature  $T$ :

$$Q = -\Delta H_R|_T = -\left(\Delta H_R|_{T_0} + \Delta H_{\text{Products}}|_{T_0 \rightarrow T} - \Delta H_{\text{Reactants}}|_{T_0 \rightarrow T}\right) \quad (11)$$

The enthalpy variations consider the  $C_p(T)$  integral and the phase transitions for each system component over each temperature path.

The general reaction kinetics is defined by the relation:

$$\mathbf{r} = H(T - T_{\text{react}})K[W_{A0}(1 - \eta_A)]^n \quad (12)$$

where  $H$  is the Heaviside function. As the reactions under study typically present very high velocities, we assume, as a first approach, zero order kinetics ( $n = 0$ ) with a non-temperature dependent  $K$ .

The dependent and independent variables are normalized by suitable parameters:

$$T^* = T/T'; \quad W_A^* = W_A/W_{A0}; \quad r^* = r/R; \quad t^* = t/\tau \quad (13)$$

The thermophysical properties are assumed to vary with temperature and composition of the mixture. Noting the component E as air in the mixture, the mixing rules for each property are defined as:

$$C_{pM} = \sum_i \omega_i C_{pi} \quad i = A, B, C, D, E \quad (14); \quad \rho_M = 1 / \sum_i \frac{\omega_i}{\rho_i} \quad i = A, B, C, D, E \quad (15)$$

$$k_M = \left(1 / \sum_i \frac{v_i}{k_i} + \sum_i v_i k_i\right) / 2 \quad i = A, B, C, D, E \quad (16); \quad \varepsilon_M = \sum_i v_i \varepsilon_i \quad i = A, B, C, D, E \quad (17)$$

where  $\omega_i$  and  $v_i$  are the mass and volumetric fractions of component  $i$  in the mixture. The conductivity of the reaction mixture (Eq. 16) is considered to be the average value between the conductivity of a serial and a parallel rearrangement of the components on a very narrow film (thickness  $\Delta r$ ) centered on each spatial node position. We introduce an equivalent conductivity component for the radiation on the void spaces in air conductivity estimative ( $k'_E$ ) of the serial arrangement:

$$k'_E = k_E + 4\sigma\varepsilon_M T^3 v_E \Delta r \quad (18)$$

Phase transitions for the several components are also considered. The transitions are introduced by adding the latent heat to the  $C_p$  estimative of a component each time the temperature crosses its transition temperatures. They occur over a temperature range ( $\Delta T$ ) of 1 K.

$$C'_{pi} = C_{pi} + L_i / \Delta T \quad (19)$$

The particular system simulated in this work is the  $\text{Fe}_2\text{O}_3/\text{Al}$  thermite. The thermophysical data for the components involved are resumed in Tables 1 and 2. Other general data is presented in Table 3.

Table 1 – General thermophysical data for the thermite system components.

Comp.	Mol. Weight (kg/mol)	Fusion Temp. (K)	Fusion Latent Heat (J/kg)	Mass Stoich. Coeff.
A - $\text{Fe}_2\text{O}_3$	0.159692	1735* (a)	-	-1
B - Al	0.026982	933 (b)	387672.46 (b)	-0.33792
C - Fe	0.055847	1809 (c)	271955,88 (c)	0.69943
D - $\text{Al}_2\text{O}_3$	0.101961	2327 (c)	1161295,74 (c)	0.63848
E - Air	0,028810	-	-	-

\* Decomposes to  $\text{Fe}_3\text{O}_4$ ; (a)–JANAF (1971); (b)–Kubaschewski and Evans (1958); (c)–Chase (1998).

### 3 Adaptive Numerical Method

The model described above is numerically solved with an adaptive strategy based on successive refinement of a initial one-dimensional spatial grid (*Grid Refinement Method* – GRM). The adaptive algorithm is applied on subproblems generated by subgrid selection procedure. In each time step, this selection is done by the comparison of the problem solution obtained over two spatial grids: a coarse one (refinement level 1) and a fine one (refinement level 2), constructed by the bisection of the

Table 2 – Temperature dependence of thermophysical properties.

Property	Comp.	Temp. Range (K) or Phys. State	Correlation	Ref.
$C_p$ $J/(kg.K)$	Al	Solid	$(4.94+2.96 \times 10^{-3}T) \times 4.184/M_{Al}$	(b)
		Liquid	$7 \times 4.184/M_{Al}$	(b)
	Fe <sub>2</sub> O <sub>3</sub>	[290-950]	$(93.43834+108.3577 \times Tr-50.86447 \times Tr^2+25.58683 \times Tr^3-1.61133 \times Tr^4)/M_{Fe2O3}$	(c)
		[950-1050]	$150.624/M_{Fe2O3}$	(c)
		[1050-1750]	$(110.9362+32.04714 \times Tr-9.192333 \times Tr^2+0.901506 \times Tr^3+5.433677 \times Tr^4)/M_{Fe2O3}$	(c)
	Fe	[290-700]	$(18.42868+24.64301 \times Tr-8.91372 \times Tr^2+9.664706 \times Tr^3-0.012643 \times Tr^4)/M_{Fe}$	(c)
		[700-1042]	$(-57767.65+137919.7 \times Tr-122773.2 \times Tr^2+38682.42 \times Tr^3+3993.08 \times Tr^4)/M_{Fe}$	(c)
		[1042-1100]	$(-325.8859+28.92876 \times Tr+411.9629 \times Tr^2)/M_{Fe}$	(c)
		[1100-1809]	$(-776.7387+919.4005 \times Tr-383.7184 \times Tr^2+57.08148 \times Tr^3+242.1369 \times Tr^4)/M_{Fe}$	(c)
	Al <sub>2</sub> O <sub>3</sub>	Solid	$(102.429+38.7498 \times Tr-15.9109 \times Tr^2+2.628181 \times Tr^3-3.007551 \times Tr^4)/M_{Al2O3}$	(c)
		Liquid	$192.464/M_{Al2O3}$	(c)
Air	-	$1.6006 \times 10^{-10}T^4 - 7.5229 \times 10^{-7}T^3 + 1.1912 \times 10^{-3}T^2 - 5.2612 \times 10^{-1}T + 1.0796 \times 10^3$	(d)**	
$\rho$ $kg/m^3$	Al	Solid	$-6.518 \times 10^{-5}T^2 - 1.478 \times 10^{-1}T + 2.751 \times 10^3$	(e)**
		Liquid	$-0.275 \times T + 2638.3$	(e)**
	Fe <sub>2</sub> O <sub>3</sub>	Solid	5062.3	Exper.
	Fe	Solid	$-1.3828 \times 10^{-7}T^3 + 3.3890 \times 10^{-4}T^2 - 5.3873 \times 10^{-1}T + 7.9929 \times 10^3$	(e)**
		Liquid	7030	(e)
	Al <sub>2</sub> O <sub>3</sub>	-	3975	(f)
Air	-	$P \times M_{air}/(R \times T)$	-	
$K$ $W/(m.K)$	Al	Solid	$2.0282 \times 10^{-7}T^3 - 4.4314 \times 10^{-4}T^2 + 2.5395 \times 10^{-1}T + 1.9586 \times 10^2$	(g)**
		Liquid	$0.03 \times T + 63$	(g)**
	Fe <sub>2</sub> O <sub>3</sub>	Solid	0.59	(h)
	Fe	[250-1200]	$4.5411 \times 10^{-5}T^2 - 1.2604 \times 10^{-1}T + 1.1394 \times 10^2$	(g)**
		[1200-	$15.231 \ln(T) - 79.556$	(g)**
	Al <sub>2</sub> O <sub>3</sub>	[250-1500]	Linear interpolation of literature data	(i)
		[1500-	$6 \times 10^{-7}T^2 - 0.0023T + 7.5$	(j)**
Air	-	$2.452 \times 10^{-14}T^4 - 9.939 \times 10^{-11}T^3 + 1.281 \times 10^{-7}T^2 + 4.456 \times 10^{-6}T + 1.369 \times 10^{-2}$	(j)**	
$\varepsilon$	Al	Solid	$2.018 \times 10^{-4}T + 1.632 \times 10^{-2}$	(g)**
		Liquid	$1.667 \times 10^{-4}T - 4.217 \times 10^{-2}$	(g)**
	Fe <sub>2</sub> O <sub>3</sub>	Solid	Linear interpolation of literature data	(k)
	Fe	Solid	0.35	(g)
		Liquid	0.37	(g)
	Al <sub>2</sub> O <sub>3</sub>	-	$9.742 \times 10^{-8}T^2 - 5.284 \times 10^{-4}T + 9.736 \times 10^{-1}$	(i)**
Air	-	$\approx 0$	-	

Tr=T/1000; \*\* Obtained by regression using data of the reference. (b),(c)–vd. Table 1; (d)– Hand. Heat Transfer (1973); (e)–Perry’s (1997); (f)–Thorpe’s (1937); (g)–CRC (1973); (h)–Lange’s (1973); (i)–HEDH (1983); (j)–Incropera and DeWitt (1990); (k)–Bejan (1993).

Table 3 – General data for the simulations.

$U_{steel/air}$ ( $W/(m^2.K)$ )	4.96	$v_{air0}$	0.40	$T_0$ (K)	298.15
$U_{PMMA/air}$ ( $W/(m^2.K)$ )	3.91	$\omega_{A0}$	0.747	$P$ (Pa)	101325
$U'_{steel/air}$ ( $W/(m^2.K)$ )	5.94	$\omega_{B0}$	0.253	$\tau$ (s)	0.1
$-\Delta H_R _{T_0}$		$T_{igni}$ (K)	2000	$T'$ (K)	1000
$K$ ( $kg/(m^3.s)$ )	variable	$t_{igni}$ (s)	variable	$R$ (m)	0.025
$R$ ( $J/(mol.K)$ )	8.31441	$T_{react}$ (K)	1200	$R_0$ (m)	0.0015
$\sigma$ ( $W/(m^2.K^4)$ )	$5.67051 \times 10^{-8}$	$\Delta r$ (m)	$1 \times 10^{-5}$	$Z$ (m)	0.010

intervals of the first grid. The nodes where the error criterion is not verified are grouped in subgrids over which subproblems are generated and solved. In each grid, the spatial derivatives are estimated by non-uniform finite difference approximations and the time integration is performed by numerical integrator DDASSL. The error criterion is defined by the difference between the values of the solution obtained by integration over two consecutive level grids, for a constant time step. The overall profiles

for the variables on all subgrids are completed by interpolation of the known values. Therefore the subgrid selection procedure is repeated until the error criterion is verified on every node of every grid or a predefined maximum refinement level is reached. In this case, the procedure is repeated with a smaller time step. For each subproblem, there are introduced artificial Dirichlet boundary conditions on each internal boundary, defined by the solution values obtained by integration of lower level subproblems. With this procedure, we prevent the occurrence of discontinuities between solution profiles obtained on grids of different levels.

#### 4 Results and Conclusions

The numerical parameters are: DDASSL tolerance –  $1 \times 10^{-5}$ , adaptive algorithm tolerance –  $1 \times 10^{-2}$ . We use a uniform first level grid with 21 nodes, cubic splines with 5 points interpolations and 5 point centered finite differences discretizations. As the procedure for dealing with boundary conditions on subgrids of level greater than 2 can eventually introduce significant errors for some type of problems, we adapt the algorithm to execute temporal step adaptation, fixing the maximum refinement level as 2. Decreasing the adaptive algorithm tolerance, we conclude that it does not affect significantly the results, only leading to greater execution times.

In a first approach, we fix all the thermophysical properties for the initial conditions of the problem. In addition, conductivity is set considering only the parallel configuration. From the performed runs, it can be stated that once the ignition time ( $t_{igni}$ ) is sufficient to induce self-propagation, the increase of its value does not affect the obtained results. We set it near the minimum value –  $t_{igni} = 0,0225$  s.

With the above conditions we verify that there is a minimum  $K$  value for self-propagation of the combustion wave ( $K_{min} = 6 \times 10^4 \text{ kg}/(\text{m}^3 \cdot \text{s})$ ). The profiles obtained with selected  $K$  values are presented in Fig. 1 and 2. All the runs are done with a fixed final time  $t^*_{fin} = 1.5$  to evidence the differences between the propagation velocities. So, in cases (b) and (c) the wave does not reach the external boundary. We conclude that increasing  $K$  leads to higher maximum temperatures and wave propagation velocities, with complete conversion in all cases. Apart from the boundary regions, the wave propagation velocities assume a constant value: (a)  $\sim 0.2$ , (b)  $\sim 0.1$ , (c)  $\sim 0.06$  m/s. This last value is in good agreement with the experimental results found by Durães et al. (2005).

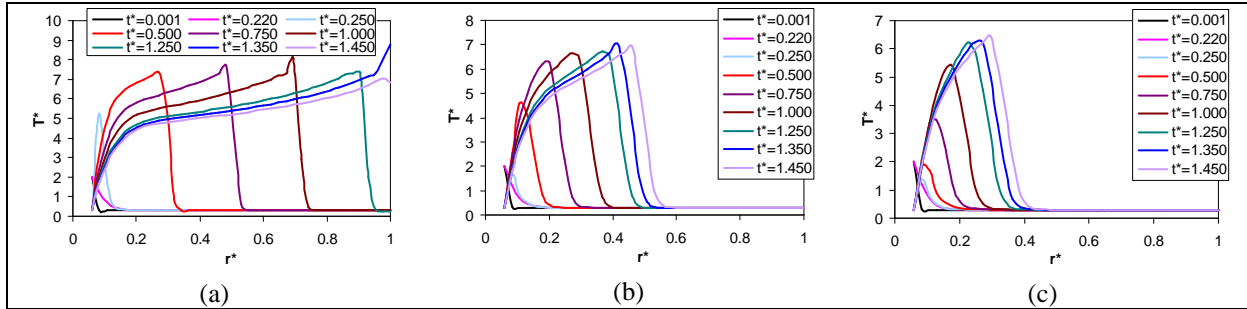


Figure 1 – Profiles for normalized temperature for (a)  $K=5 \times 10^5$ , (b)  $K=1 \times 10^5$  and (c)  $K=6 \times 10^4 \text{ kg}/(\text{m}^3 \cdot \text{s})$ .

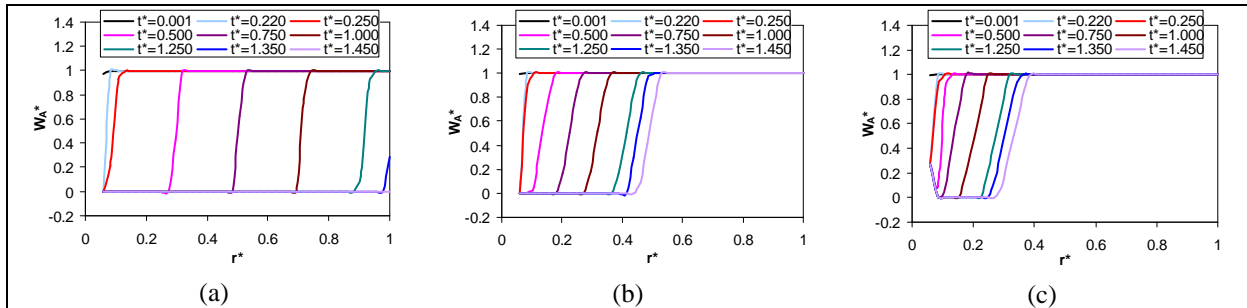


Figure 2 – Profiles for normalized concentration for (a)  $K=5 \times 10^5$ , (b)  $K=1 \times 10^5$  and (c)  $K=6 \times 10^4 \text{ kg}/(\text{m}^3 \cdot \text{s})$ .

After the activation of the thermophysical properties variation (one at a time), we find numerical difficulties in all cases, except for the emissivity (which does not affect significantly the results).

These problems can be due to convergence difficulties of the BDF implicit temporal integration method (in DDASSL) that arise always at a determinate temporal level and may be explained by the accumulation of round-off errors. For times lower than crash time, it is possible to identify a self-propagation wave, characterized by lower maximum temperatures, indicating that these would be more realistic simulations. To overcome these problems a further tuning of the numerical parameters is under way, combined with a more intensive monitoring of property values evolution.

## References

- Bejan, A. (1993). *Heat Transfer*, John Wiley, New York.
- Bowen, C.R., Derby, B. (1995). Finite-difference modelling of self-propagating high-temperature synthesis of materials. *Acta Metall. Mater.*, 43 (10), 3903-1913.
- Brito, P. (1998). *Aplicação de métodos numéricos adaptativos na integração de sistemas algébrico-diferenciais caracterizados por frentes abruptas*, MSc. Thesis, DEQ-FCTUC, Coimbra, Portugal.
- Brito, P., Durães, L., Campos, J., Portugal, A. (2004). Aplicação de métodos adaptativos para a simulação de processos de combustão. in Proc. of Congresso de Métodos Computacionais em Engenharia, APMTAC & SEMNI & LNEC, Lisboa, 472 & CD-ROM.
- Carrillo-Heian, E.M., Graeve, O.A., Feng, A., Faghieh, J.A., Munir, Z.A. (1999). Modeling studies of the effect of thermal and electrical conductivities and relative density of field-activated self-propagating combustion synthesis. *J. Mater. Res.*, 14 (5), 1949-1958.
- Chase, M., Jr. (1998). NIST-JANAF Thermochemical Tables, 4<sup>th</sup> ed., *J. Phys. Chem. Ref. Data*, Mon. 9, 1-1951.
- CRC Handbook of Chemistry of Physics* (1973), 54<sup>th</sup> ed., CRC Press, Cleveland.
- Cuadrado-Laborde, C., Damonte, L.C., Mendoza-Zélis, L. (2003). Theoretical treatment of a self-sustained, ball milling induced, mechanochemical reaction in the Fe<sub>2</sub>O<sub>3</sub>-Al system, *Mater. Sci. & Eng.*, A355, 106-113.
- Durães, L., Campos, J., Portugal, A. (2005). Radial combustion propagation in iron(III) oxide/aluminum thermite mixtures, *Propell. Explos. Pyrot.*, accepted for publication.
- Graeve, O.A., Carrillo-Heian, E.M., Feng, A., Munir, Z.A. (2001). Modeling of wave configuration during electrically ignited combustion synthesis. *J. Mater. Res.*, 16 (1), 93-100.
- Handbook of Heat Transfer* (1973), McGraw-Hill, New York.
- HEDH – Heat Exchange Design Handbook* (1983), Hemisphere Publishing Corporation, Washington.
- Incropera, F., DeWitt, D. (1990). *Fundamentals of Heat and Mass Transfer*, 3<sup>rd</sup> ed., John Wiley, NY.
- Ivleva, T.P., Merzhanov, A.G. (2000). Three-dimensional spinning waves in the case of gas-free combustion. *Doklady Phys.*, 45 (4), 136-141.
- JANAF Thermochemical Tables* (1971), 2<sup>nd</sup> ed., National Bureau of Standards (US), Washington.
- Kubaschewski, O., Evans, E. (1958). *Metallurgical Thermochemistry*, 3<sup>rd</sup> ed. rev., Pergamon Press, London.
- Lange's Handbook of Chemistry* (1973), 11<sup>th</sup> ed., McGraw-Hill, New York.
- Makino, A. (2001). Fundamental aspects of the heterogeneous flame in the self-propagating high-temperature synthesis (SHS) process. *Prog. Energy & Comb. Sci.*, 27, 1-74.
- Moore, J.J., Feng, H.J. (1995). Combustion synthesis of advanced materials: Part II. Classification, applications and modelling. *Prog. Mater. Sci.*, 39, 275-316.
- Norozhilov, B.V. (1992). Non-linear SHS phenomena: experiment, theory, numerical modelling. *Pure & Appl. Chem.*, 64 (7), 955-964.
- Perry's Chemical Engineers' Handbook* (1997), 7<sup>th</sup> ed., Mc-Graw-Hill, New York.
- Raymond, C.S., Shkadinsky, K.G., Volpert, V.A. (1998). Gravitational effects on liquid flame thermite systems. *Comb. Sci. & Tech.*, 131, 107-129.
- Shkadinsky, K.G., Shkadinskaya, G.V., Matkowski, B.J. (2000). Gas-phase influence on quasisteady “liquid flames” in gravitational fields, *Comb. Sci. & Tech.*, 157, 87-110.
- Shkadinsky, K.G., Shkadinskaya, G.V., Volpert, V.A. (1997). Stability of “liquid flame” combustion waves, *Chem. Eng. Sci.*, 52 (9), 1415-1428.
- Thorpe's Dictionary of Applied Chemistry* (1937), 4<sup>th</sup> ed., Vol. I, Longmans, London.
- Volpert, V.A., Volpert, V.I., Davtyan, S.P., Megrabova, I.N., Surkov, N.F. (1992). Two dimensional combustion modes in condensed flow. *SIAM J. Appl. Math.*, 52 (2), 368-383.